A simple tight-binding model for the study of 4d transition metals under pressure

C. Cazorla [a,*], D. Alfè [b,c,d,e], M.J. Gillan [c,d,e]

[a] Institut de Ciència de Materials de Barcelona (ICMAB-CSIC), 08193 Bellaterra, Spain
[b] Dept. of Earth Sciences, University College London, London WC1E 6BT, UK
[c] Thomas Young Centre at University College London, London WC1E 6BT, UK
[d] London Centre for Nanotechnology, University College London, London WC1H 0AH, UK
[e] Dept. of Physics and Astronomy, University College London, London WC1E 6BT, UK

ARTICLE INFO

ABSTRACT

Recently we have developed a simple tight-binding (TB) model of transition metals in the region near the middle of the 4d-series tuned to mimic molybdenum. The energetic, structural and melting properties deriving from this model are quite close to those obtained in previous first-principles work on Mo. TB approaches, reasonably accurate but computationally less demanding than first-principles calculations, therefore can be used to perform systematic analysis on the physical properties of transition metals across the 4d-series over wide thermodynamic ranges. Here we present a series of TB parametrizations designed to emulate the behavior of niobium, technetium, ruthenium, rhodium and palladium under extreme conditions of pressure and temperature. Our simple TB model is composed of two basic contributions to the energy: first, the pairwise repulsion due to Fermi exclusion, and second, the d-band bonding energy described in terms of an electronic density of states that depends on structure. The parameters of the model are adjusted to fit the dependence on pressure of the d-band width and the zero-temperature equation of state of the element in question. Calculated TB phonon spectra compare very well with ab initio results and experimental data, and the stable crystal structure in all transition metals at equilibrium is correctly predicted.

© 2011 Elsevier B.V. All rights reserved.

1. Introduction

The physics of transition metals (TM) at low temperatures and pressures is well understood as result of an early combination of experiments, first-principles calculations and simple models [1–4]. Recent advances on experimental techniques and first-principles calculations might lead to similar understanding of TM at high temperatures and Mbar pressures but present information on the phase diagrams of interest is rather fragmentary and conflicting [5–9]. Many years ago, shock wave (SW) measurements provided the first experimental $P - T$ points on the melting lines of TM (Fe, Mo, Ta and W) in the Mbar regime [10,11]; lately, static compression techniques based on the diamond anvil cell (DAC) were used to fully map out the solid–liquid phase boundary of Fe, Mo, Ta, W, V and Y at pressures and temperatures up to ∼100 GPa and ∼4000 K [12]. Strikingly, huge discrepancies appeared among the sets of SW and DAC melting data amounting to several thousand K in some cases and DAC providing always the lowest melting curves. On the theoretical side, modeling of melting curves from first-principles (FP) started more than 10 years ago [13,14]. Metals like Fe, Mo and Ta have been investigated with these techniques and so far FP calculations appear to support the correctness of SW measurements. Some explanations based on quite diverse arguments have been proposed in order to rationalize the origins of such dramatic disagreements, however, general consensus on this matter still lacks within the high-pressure research community.

In a recent work [15] we have developed a simple tight-binding (TB) model for transition metals with parameters tuned to mimic molybdenum at high pressures and which reproduces closely previous first-principles results. In general, TB approaches are reasonably accurate and computationally less demanding than FP calculations so that one can use them to map out systematic trends in elements of a same family. Here, we present a series of TB parametrizations based on the same simple model as introduced in [15] and designed to render the behavior of niobium, technetium, ruthenium, rhodium and palladium under extreme thermodynamic conditions. It is our intention to use these models in the near future to study systematically the melting properties of 4d-TM and so help to resolve the conflicting discrepancies cited above. Besides of this our aim, the TB potentials presented in this article may be useful to other researchers who pursue to perform studies on TM which typically are computationally very expensive with FP techniques (e.g. energetics of crystal defects, molecular dynamics simulations and reproduction of shock-wave compression effects

* Corresponding author. Tel.: +34 605958137.
  E-mail address: ccazorla@icmab.es (C. Cazorla).

Table 1
TB parameters tuned to reproduce the behavior of 4d-TM from equilibrium up to pressures of 400 GPa.

Element	A_r (eV)	R_r (Å)	A_b (eV)	R_b (Å)	N_d
Nb (bcc)	817.1988	0.4250	14.5720	1.0134	3.4
Mo (bcc)	3164.3454	0.3350	18.5745	0.8950	4.3
Tc (hcp)	3736.5815	0.3200	18.2814	0.8500	5.7
Ru (hcp)	10388.3830	0.2800	53.7246	0.6200	6.9
Rh (fcc)	20997.6673	0.2500	146.8910	0.4850	8.5
Pd (fcc)	69254.1517	0.2150	202.5752	0.4500	9.7

in matter, to name a few). The results presented in this modeling work, therefore, are of interest to a broad scientific audience.

The remainder of this article is organized as follows. In Section 2, we summarize the methodology and technicalities in our calculations. Next, we present our TB modeling results on 4d-TM elements and finalize by providing the discussion and conclusions in Section 4.

2. Method and technicalities

Details of our TB model and fitting procedure are reported in [15] so here we just review the essential ideas. The total energy U_{tot} for a system of N atoms with positions $\mathbf{r}_i$ is expressed as :

$$U_{tot}(\mathbf{r}_1, \mathbf{r}_2, \ldots, \mathbf{r}_N) = \frac{1}{2} \sum_{i \neq j} V_{REP}(r_{ij}) + U_{TB}(\mathbf{r}_1, \mathbf{r}_2, \ldots, \mathbf{r}_N), \quad (1)$$

where $r_{ij} = |\mathbf{r}_i - \mathbf{r}_j|$, $V_{REP}(r) = A_r \exp(-r/R_r)$ is a pairwise potential representing the electronic repulsion due to Fermi exclusion and U_{TB} stands for the attractive d-band bond energy and electronic thermal effects. In order to simplify the calculations, we consider only electronic d-band states (i.e., xy, yz,zx, $x^2 + y^2$ and $3z^2 - r^2$) in the TB Hamiltonian matrix elements $\langle i\alpha|H|j\beta \rangle$ and assume the canonical ratios $dd\sigma:dd\pi:dd\delta = -6:4:-1$ on them. TB matrix elements $\langle i\alpha|H|j\beta \rangle$ represent hopping integrals between electronic d-orbitals α and β centred in atoms i and j, respectively, and they are assumed to decrease exponentially with the interatomic distance r_{ij} according to $A_b \exp(-r_{ij}/R_b)$. The zero-temperature value of the d-band bond energy U_{TB} corresponds to the sum of single-electron energies spanned over occupied states that is obtained from direct diagonalization of the TB Hamiltonian matrix; finite-temperature effects then can be included using the Fermi–Dirac occupation distribution function and expression of the electronic entropy. To fix the value of parameters A_b and R_b we require the second moment of the TB density of states (DOS) to agree with the volume dependent d-band

second moment as obtained with DFT. In order to reproduce the energy difference between the Fermi level E_F and bottom of the d-band we also treat the number of d-electrons N_d as an adjustable parameter [16]. With the value of parameters A_b, R_b and N_d fixed, parameters A_r and R_r are chosen so as to reproduce as closely as possible the $P(V)$ curve obtained with DFT and experimental data whenever possible. In all cases, cut-off distances for the atomic pairwise interactions are set to $R_{cut} = 4.9$ Å. To apply this procedure, we have performed DFT calculations using the full-potential linearized augmented plane-wave method (FP-LAPW) as implemented in the WIEN2k code [17] and with the generalized gradient approximation for the exchange-correlation energy due to Wu and Cohen [18]. Technical parameters in our calculations have been set so as to ensure convergence of the total energy to less than 1 meV/atom. A pressure interval of 400 GPa has been considered throughout our analysis. We refer the interested reader to works [4,15] where full details of our FP-LAPW and TB calculations are provided.

3. Results

In Table 1, we report the value of the TB parameters that better reproduce the behavior of Nb, Mo, Tc, Ru, Rh and Pd at equilibrium and high pressures according to the strategy explained in the previous section. As can be seen from Figs. 1 and 2, very good agreement between these simple models and first-principles calculations (coinciding with experimental data) is achieved for the zero-temperature equation of state. With regard to the electronic d-band features, in Mo for example the second moment of the DFT d-DOS (see Tables 2 and 3) amounts to 7.2 (23.7) eV^2 at zero-pressure ($P = 350$ GPa) while the value of the corresponding TB d-DOS is 7.3 (21.3) eV^2. The energy difference between the Fermi energy level and bottom of the d-band at zero pressure ($P = 350$ GPa) is calculated to be 5.9 (10.8) and 5.9 (10.9) eV with DFT and TB, respectively. Equivalent good TB reproducibility of DFT d-band energy results is found also in the rest of TM considered (see Tables 2 and 3).

In order to assess the reliability of the TB parametrizations introduced in this work we calculated the vibrational phonon spectrum of Mo, Tc and Pd at the corresponding experimental equilibrium volumes, and compared them with DFT calculations of our own and room-temperature experimental data. DFT phonon frequencies were obtained using the projector augmented-wave (PAW) technique as given by the VASP code [22], exchange-correlation energy approximation due to Perdew et al. [23], and the atomic small-displacement method as implemented in the PHON code [24]. A simulation supercell containing 64(96) particles was used for the phonon calculations in the bcc and
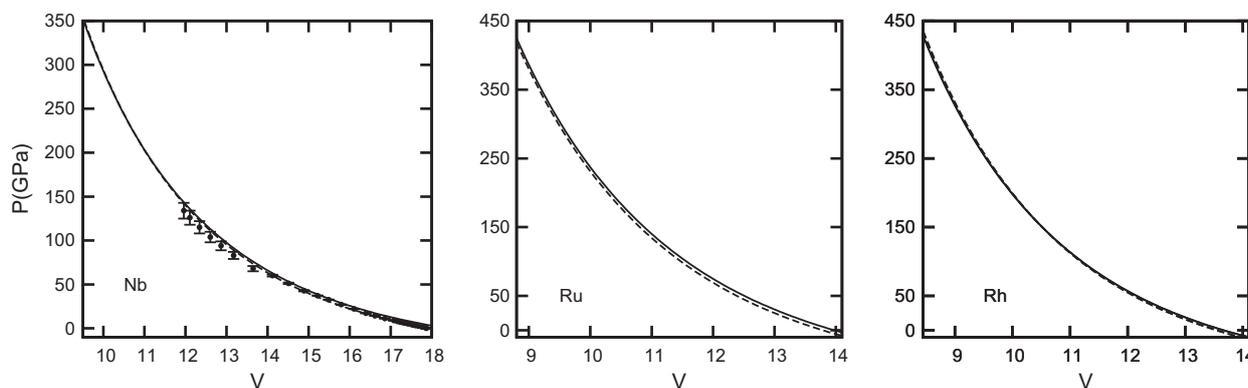

Fig. 1. Zero-temperature equation of state of Nb, Ru and Rh as obtained with the TB model and parametrizations presented in this work (solid lines). Calculated DFT $P(V)$ curves (dashed lines) and experimental data (dots) from Ref. [19] are shown for comparison. Volume is units of Å^3 per atom.
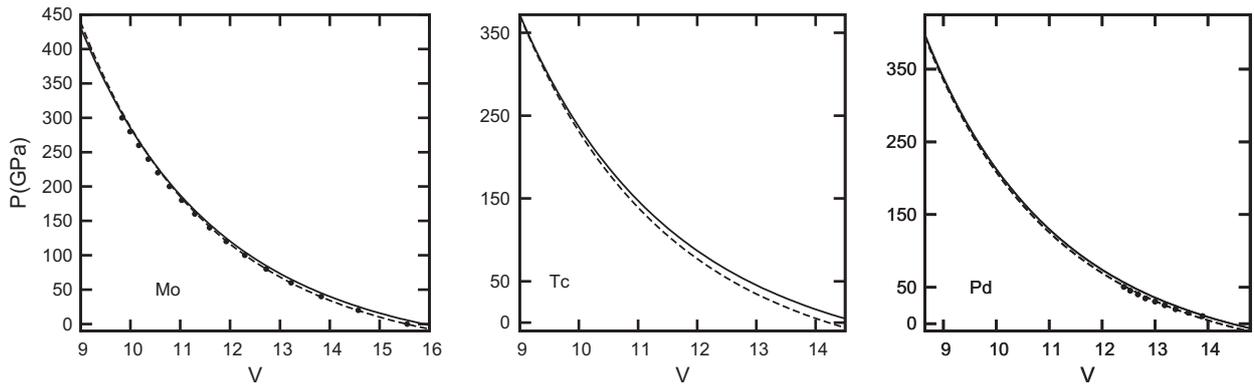
Fig. 2. Zero-temperature equation of state of Mo, Tc and Pd as obtained with the TB model and parametrizations presented in this work (solid lines). Calculated DFT $P(V)$ curves (dashed lines) and experimental data (dots) from Refs. [20,21] are shown for comparison. Volume is units of Å^3 per atom.

Table 2

TB (DFT) d-band features calculated at zero-pressure. The d-band width is defined as $W_d = E_d^t - E_d^b$, where E_d^t and E_d^b are the top and bottom single-electron energy levels, respectively. The second d-band moment is defined as $\mu^{(2)} = \int_{-\infty}^{\infty} (\epsilon - \mu^{(1)})^2 g(\epsilon) d\epsilon / N$, where ϵ represents the single-electron energy spectrum, $g(\epsilon)$ the Fermi–Dirac occupation distribution function, $\mu^{(1)} = \int_{-\infty}^{\infty} \epsilon g(\epsilon) d\epsilon / N$ and $N = \int_{-\infty}^{\infty} g(\epsilon) d\epsilon$.

Element	E_d^b (eV)	E_d^t (eV)	W_d (eV)	$\mu^{(2)}$ (eV^2)
Nb (bcc)	−5.5 (−4.1)	5.0 (6.1)	10.5 (10.2)	7.1 (7.1)
Mo (bcc)	−6.3 (−5.6)	4.8 (4.8)	11.1 (10.4)	7.3 (7.2)
Tc (hcp)	−5.5 (−6.8)	4.0 (3.2)	9.5 (10.0)	6.6 (6.5)
Ru (hcp)	−6.3 (−5.6)	4.8 (5.0)	11.1 (10.6)	7.3 (7.2)
Rh (fcc)	−5.1 (−7.0)	3.5 (2.3)	8.6 (9.3)	5.5 (5.2)
Pd (fcc)	−6.3 (−5.6)	4.8 (4.9)	11.1 (10.5)	7.3 (7.2)

Table 3

TB (DFT) d-band features calculated at $P = 350$ GPa. The d-band width is defined as $W_d = E_d^t - E_d^b$, where E_d^t and E_d^b are the top and bottom single-electron energy levels, respectively. The second d-band moment is defined as $\mu^{(2)} = \int_{-\infty}^{\infty} (\epsilon - \mu^{(1)})^2 g(\epsilon) d\epsilon / N$, where ϵ represents the single-electron energy spectrum, $g(\epsilon)$ the Fermi–Dirac occupation distribution function, $\mu^{(1)} = \int_{-\infty}^{\infty} \epsilon g(\epsilon) d\epsilon / N$ and $N = \int_{-\infty}^{\infty} g(\epsilon) d\epsilon$.

Element	E_d^b (eV)	E_d^t (eV)	W_d (eV)	$\mu^{(2)}$ (eV^2)
Nb (bcc)	−11.0 (−10.4)	9.0 (12.2)	20.0 (22.6)	23.9 (28.5)
Mo (bcc)	−10.7 (−11.0)	7.7 (9.4)	18.4 (20.4)	21.3 (23.7)
Tc (hcp)	−9.5 (−11.0)	6.8 (6.7)	16.3 (17.7)	20.4 (24.1)
Ru (hcp)	−9.2 (−11.2)	6.5 (4.2)	15.7 (15.4)	20.1 (18.8)
Rh (fcc)	−10.0 (−12.7)	7.0 (2.2)	17.0 (14.9)	18.1 (15.4)
Pd (fcc)	−8.9 (−11.8)	6.1 (1.1)	15.0 (12.9)	14.3 (11.2)

Fig. 3. TB phonon frequencies of Mo (dashed lines) calculated at the experimental equilibrium volume. Corresponding DFT phonon spectra (solid lines) and experimental room-temperature data (dots) from Ref. [25] are shown for comparison.
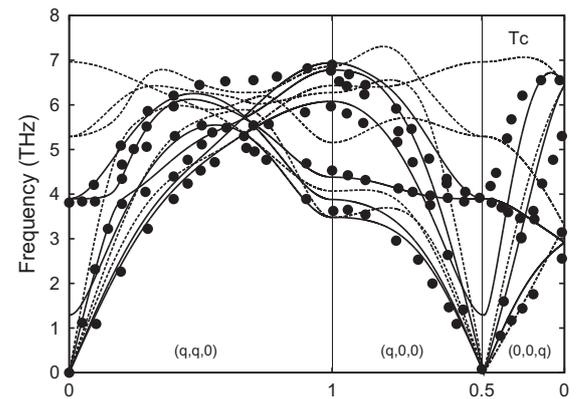
Fig. 4. TB phonon frequencies of Tc (dashed lines) calculated at the experimental equilibrium volume. Corresponding DFT phonon spectra (solid lines) and experimental room-temperature data (dots) from Ref. [26] are shown for comparison.

fcc (hcp) crystal structures. In Figs. 3–5 we plot the results of our calculations in Mo (bcc structure, $V = 15.55$ Å^3/atom), Tc (hcp structure, $V = 14.21$ Å^3/atom) and Pd (fcc structure, $V = 14.70$ Å^3/atom), respectively. In general, good TB reproducibility of the computed first-principles vibrational phonon frequencies and experimental data can be claimed.

We carried out a further test in which we analyzed the relative stability of the bcc, fcc and hcp phases in Nb, Mo, Tc, Ru, Rh and Pd at equilibrium as predicted by the present TB parametrizations. The outcomes of this test are represented in Fig. 6. It is found that the stable crystal structure is predicted correctly in all the elements considered (e.g. bcc in Nb and Mo, hcp in Tc and Ru, and fcc in Rh and Pd). Nevertheless, we note that the value of the calculated TB energy differences ΔE among the various crystal structures do not reproduce closely those obtained with DFT. For instance, the energy difference between the hcp and bcc phases in Nb amounts to 0.6 eV when calculated with DFT whereas is
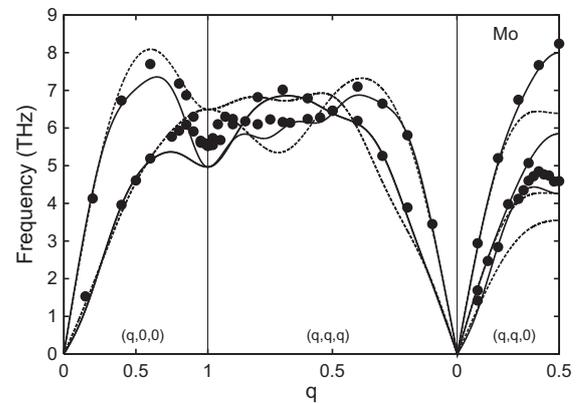
0.2 eV with TB. Seemingly, there exists a discrepancy of 0.18 eV among the TB and DFT fcc–bcc energy values calculated in Pd. This lack of agreement is not surprising since only one crystal structure per element is considered in our TB fitting strategy. We note however that reproducibility of DFT ΔE results can be improved by slightly varying the value of N_d while keeping the value of the rest of TB parameters fixed.

Fig. 5. TB phonon frequencies of Pd (dashed lines) calculated at the experimental equilibrium volume. Corresponding DFT phonon spectra (solid lines) and experimental room-temperature data (dots) from Ref. [27] are shown for comparison.
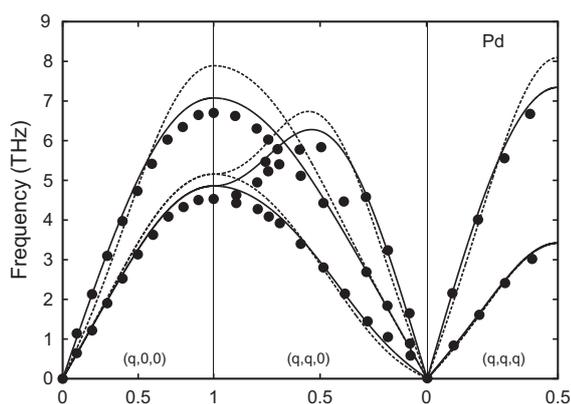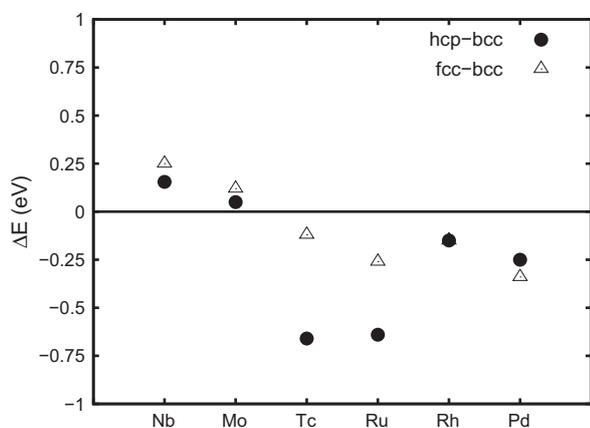

Fig. 6. Relative stability of the bcc, fcc and hcp crystal structures in 4d TM at equilibrium as calculated with the present TB model and parametrizations.

4. Discussion and conclusions

In a recent work [15], we have proved that the TB model and fitting procedure reviewed in this article can reproduce fairly the melting properties of bcc Mo obtained with first-principles methods and up to pressures of 400 GPa. In this work, we present analogous TB parametrizations for transition metals Nb, Tc, Ru, Rh and Pd and prove similar notable agreement with respect to first-principles calculations and experimental data. Therefore, it is likely that the melting properties deriving from these models can be used to map out systematic trends across the 4d-TM series with reliability while keeping the computational cost of the calculations within reasonably affordable limits. In fact, it is our intention to carry out this type of study in the near future.

The TB modeling presented in this article can be used to explore properties and physical phenomena in TM, other than melting, which simultaneously require from accurate description of the electronic d-bond features and a large number of atoms to be simulated. Examples include: the energetics and dynamics of crystalline defects (line and planar), simulation of shock-wave matter compression, modeling of ablation in metals, etc. Very interestingly, it has been proposed recently an explanation for the DAC low-temperature melting line in tantalum (also in conflict with SW data and FP calculations) based on a thermally activated and shear-induced structural transformation from bcc to an anisotropic Bingham-like plastic flow [28]. In that study, Wu et al. perform extensive non-hydrostatic molecular dynamics simulations using a many-body interatomic potential developed for applications of Ta across wide temperature and pressure ranges [29]. An interesting test which could further generalize the conclusions drawn by Wu et al. in [28] may consist in performing similar molecular dynamics simulations using the 4d-TM TB model and parametrizations provided in this manuscript. Work in this direction is already in progress.

References

[1] J. Friedel, in: The Physics of Metals, Cambridge University Press, London, 1969.
[2] J.C. Duthie, D.G. Pettifor, Phys. Rev. Lett. 38 (1977) 564.
[3] V. Heine, Phys. Rev. 153 (1967) 673.
[4] C. Cazorla, D. Alfè, M.J. Gillan, Phys. Rev. B 77 (2008) 224103.
[5] C. Cazorla, M.J. Gillan, S. Taioli, D. Alfè, J. Chem. Phys. 126 (2007) 194502.
[6] S. Taioli, C. Cazorla, M.J. Gillan, D. Alfè, Phys. Rev. B 75 (2007) 214103.
[7] D. Errandonea, Physica B 357 (2005) 356.
[8] A.B. Belonoshko, L. Burakovsky, S.P. Chen, B. Johansson, A.S. Mikhaylushkin, D.L. Preston, S.I. Simak, D.C. Swift, Phys. Rev. Lett. 100 (2008) 135701;
A.B. Belonoshko, L. Burakovsky, S.P. Chen, B. Johansson, A.S. Mikhaylushkin, D.L. Preston, S.I. Simak, D.C. Swift, Phys. Rev. Lett. 101 (2008) 049602.
[9] C. Cazorla, D. Alfè, M.J. Gillan, Phys. Rev. Lett. 101 (2008) 049601.
[10] R.S. Hixson, J.N. Fritz, J. Appl. Phys. 71 (1992) 4.
[11] A.C. Mitchell, W.J. Nellis, J. Appl. Phys. 52 (1981) 3363.
[12] D. Errandonea, B. Schwager, R. Ditz, C. Gessman, R. Boehler, M. Ross, Phys. Rev. B 63 (2001) 132104.
[13] G.A. Wijs, G. Kresse, M.J. Gillan, Phys. Rev. B 57 (1998) 8223.
[14] D. Alfè, M.J. Gillan, G.D. Price, Nature 401 (1999) 462.
[15] C. Cazorla, D. Alfè, M.J. Gillan, J. Chem. Phys. 130 (2009) 174707.
[16] A.T. Paxton, J. Phys. D 29 (1996) 1689.
[17] P. Blaha, K. Schwarz, G.K. Madsen, D. Kvasnichka, J. Luitz, WIEN2k: An Augmented Plane Wave plus Local Orbital Program for Calculating Crystal Properties, Tech. Univ. of Vienna, 2001.
[18] Z. Wu, R.E. Cohen, Phys. Rev. B 73 (2006) 235116.
[19] T. Kenichi, A.K. Singh, Phys. Rev. B 73 (2006) 224119.
[20] S. Hixson, J.N. Fritz, J. Appl. Phys. 71 (1992) 1721.
[21] H. Rice, R.G. McQueen, J.H. Walsh, Solid State Phys. 6 (1958) 1.
[22] G. Kresse, J. Furthmüller, Phys. Rev. B 54 (1996) 11169.
[23] J.P. Perdew, K. Burke, M. Ernzerhof, Phys. Rev. Lett. 77 (1996) 3865.
[24] D. Alfè, Program, 1998. <http://chianti.geol.ucl.ac.uk/~dario>;
D. Alfè, Comput. Phys. Commun. 180 (2009) 2622.
[25] Y. Nakagawa, A.D.B. Woods, Phys. Rev. 11 (1963) 271.
[26] R. Heid, L. Pintschovius, W. Reichardt, K.-P. Bohnen, Phys. Rev. B 61 (2000) 12059.
[27] Barry L. Fielek, J. Phys. F: Met. Phys. 10 (1980) 2381.
[28] C.J. Wu, P. Söderlind, J.N. Glosli, J.E. Klepeis, Nat. Mater. 8 (2009) 223.
[29] J.A. Moriarty, Phys. Rev. B 49 (1994) 12431.